

Supplementary material

Soil-plant-water relationships and crop yield under conservation agricultural practices: A biophysical basis for tailored adoption

Mosisa Tujuba Wakjira¹, Renske Hijbeek¹, Joost van Heerwaarden¹, John Koestel², Sara Bonetti³, Johan Six⁴, Katrien Descheemaeker¹

¹Plant Production Systems Group, Wageningen University and Research, 6708PB, Wageningen, The Netherlands

²Soil Quality and Soil Use, Agroscope, 8046 Zurich, Switzerland

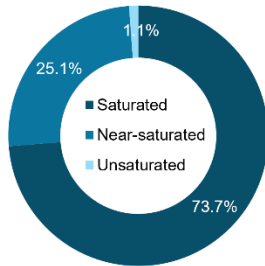
³Laboratory of Catchment Hydrology and Geomorphology, EPFL, 1951 Sion, Switzerland

⁴Institute of Agricultural Sciences, ETH Zurich, 8092 Zurich, Switzerland

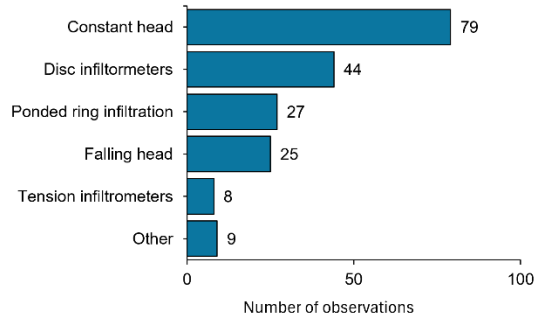
Correspondence to: Mosisa Tujuba Wakjira (mosisa.wakjira@wur.nl); or mosisatujuba@gmail.com)

Additional figures

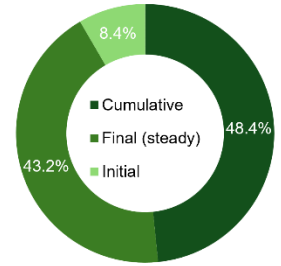
(a) Hydraulic conductivity (Kh)



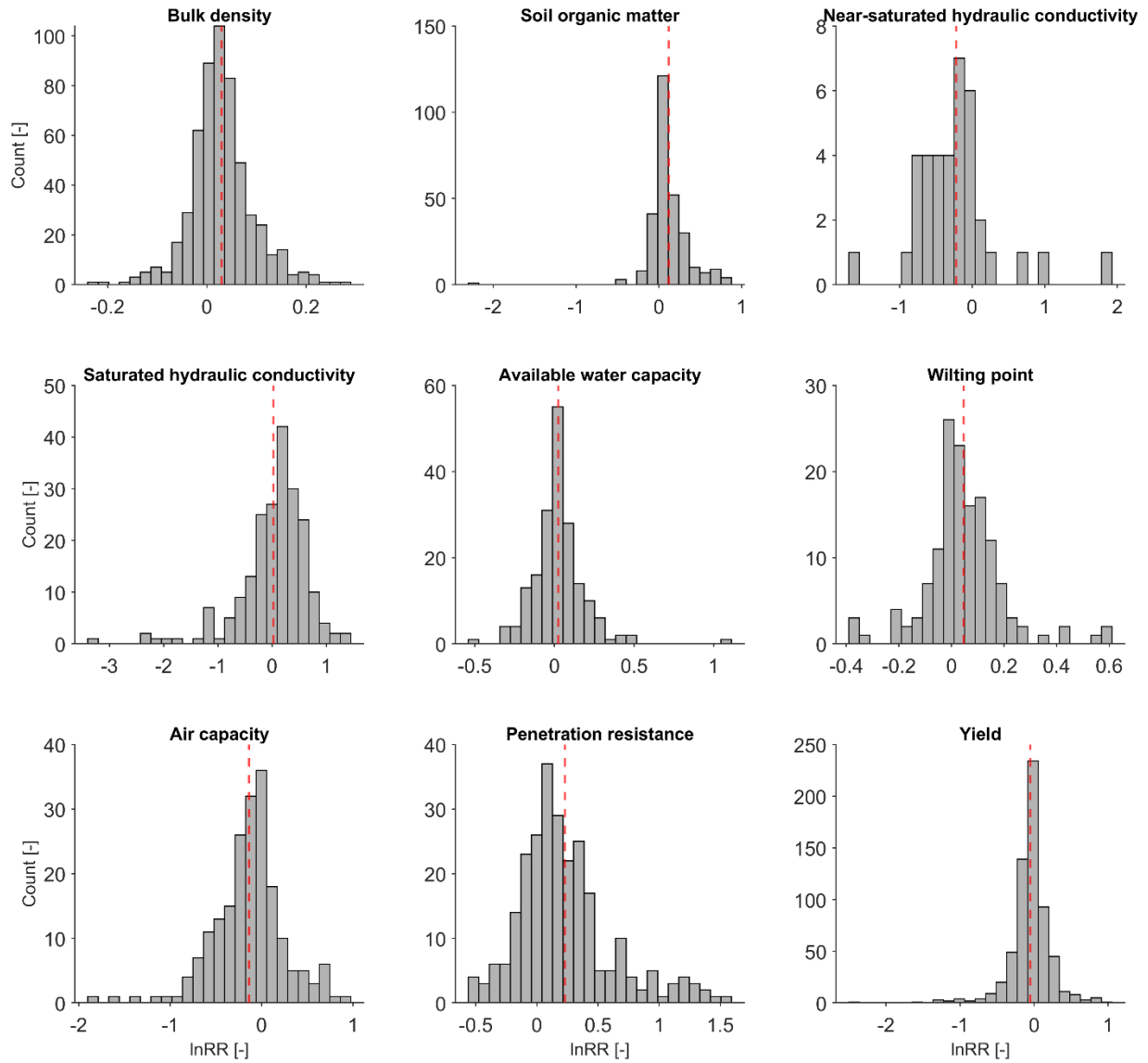
(b) Methods of Kh measurements



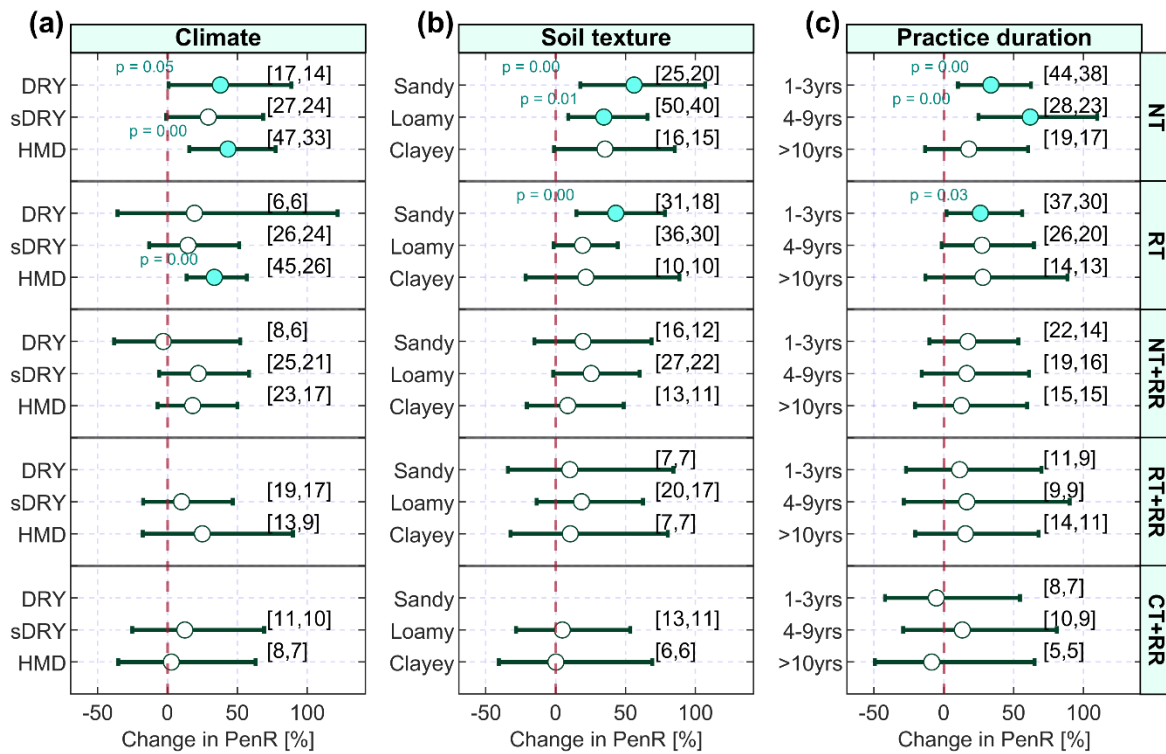
(c) Infiltration



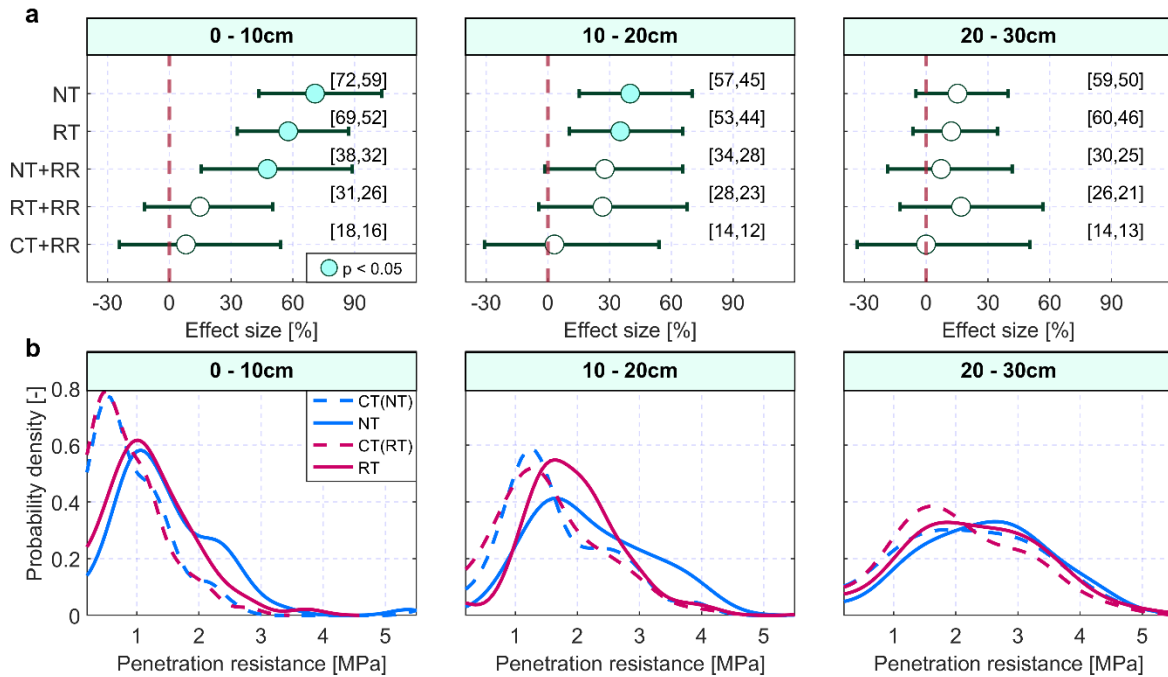
Supplementary Figure 1: Reported hydraulic conductivity and infiltration data in literature considered. (a) Types and relative proportions of hydraulic conductivity; (b) Measurement methods, by number of observations, of hydraulic conductivity. ‘Ponded infiltration’ category includes methods reported as Beerkan infiltration run and ring infiltrometer measurements. ‘Tension-disc infiltrometers’ category includes dual-head infiltrometers of various types, for example, SATURO and hood infiltrometers. ‘Other’ category includes devices such as KSAT Meter for which working principles were not described, and the HYPROP device used to measure unsaturated hydraulic conductivity; (c) Types and percentages of infiltration measured through the literature considered. Double-ring infiltrometers were the most commonly reported measurement method, followed by disc and ponded infiltrometers.



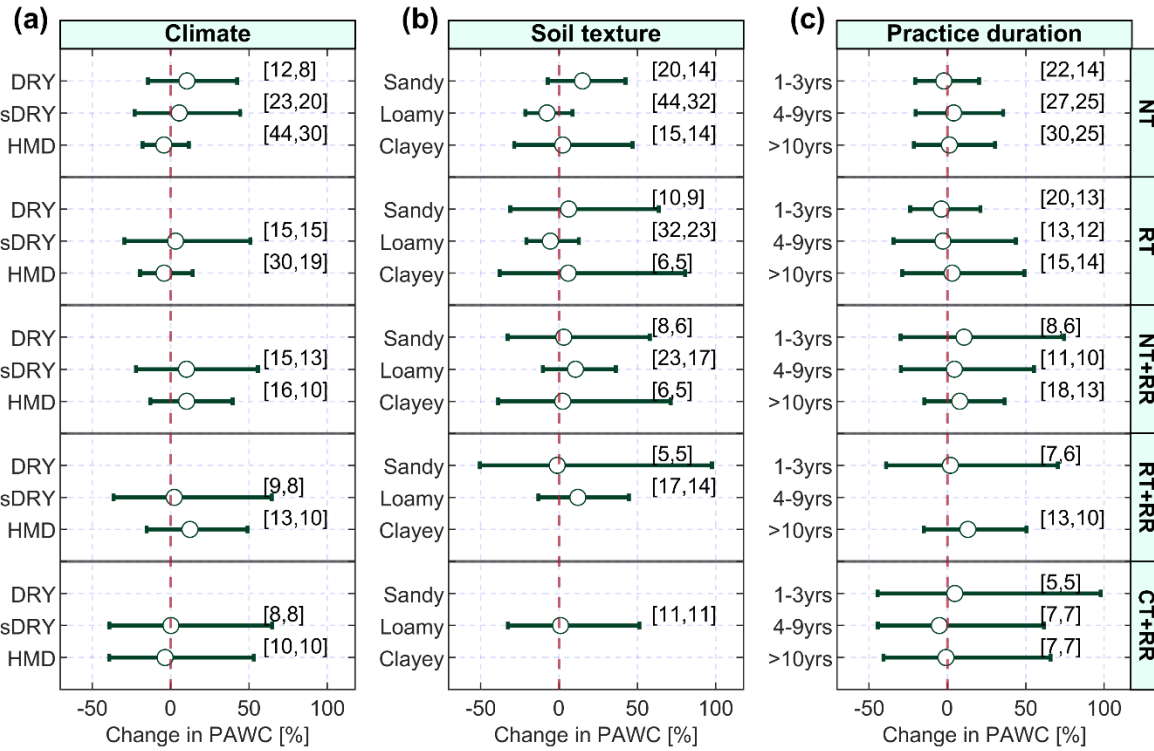
Supplementary Figure 2: Distributions of log-transformed response ratios (lnRR) for soil properties and crop yield under no-till and reduced tillage, irrespective of residue management. The red vertical line indicates the arithmetic mean lnRR.



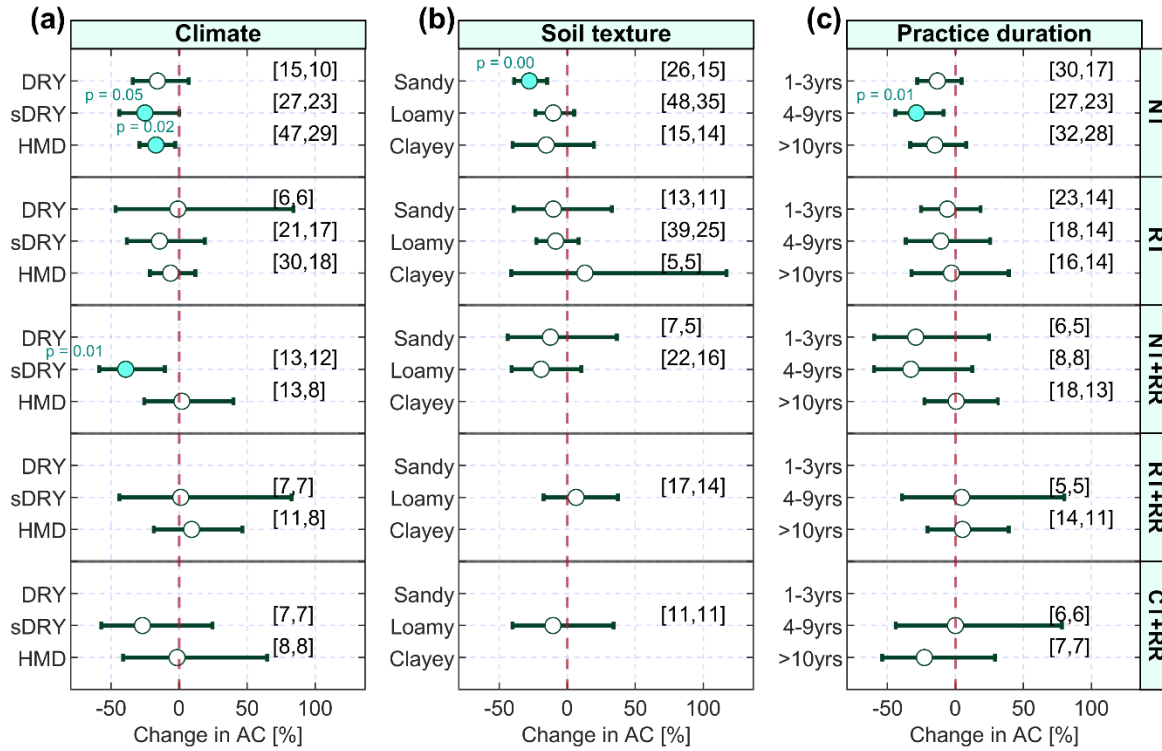
Supplementary Figure 3: Changes in soil penetration resistance (PenR) under reduced soil disturbance and residue retention. Effects of no-till (NT) and reduced tillage (RT), with (+) and without residue retention (RR) relative to conventional tillage (CT), are shown across climatic conditions (a), soil types (b), and durations of practice (c). Climate classes were defined by the aridity index (AI) as dry (DRY; AI < 0.3), semi-dry (sDRY; 0.3 < AI ≤ 0.65) and humid (HMD; AI > 0.65). Mean effects (expressed in %) are shown by circles, with horizontal bars representing 95% confidence intervals. Cyan-filled circles show statistically significant effects. Red circles indicate statistically significant trends in the effects along gradients of climatic, soil texture or duration moderators. Dashed red vertical lines represent no effect relative to CT. Numbers in square brackets indicate the number of observations (first) and studies (second) included in each analysis. Only results based on observations from at least 5 studies are shown.



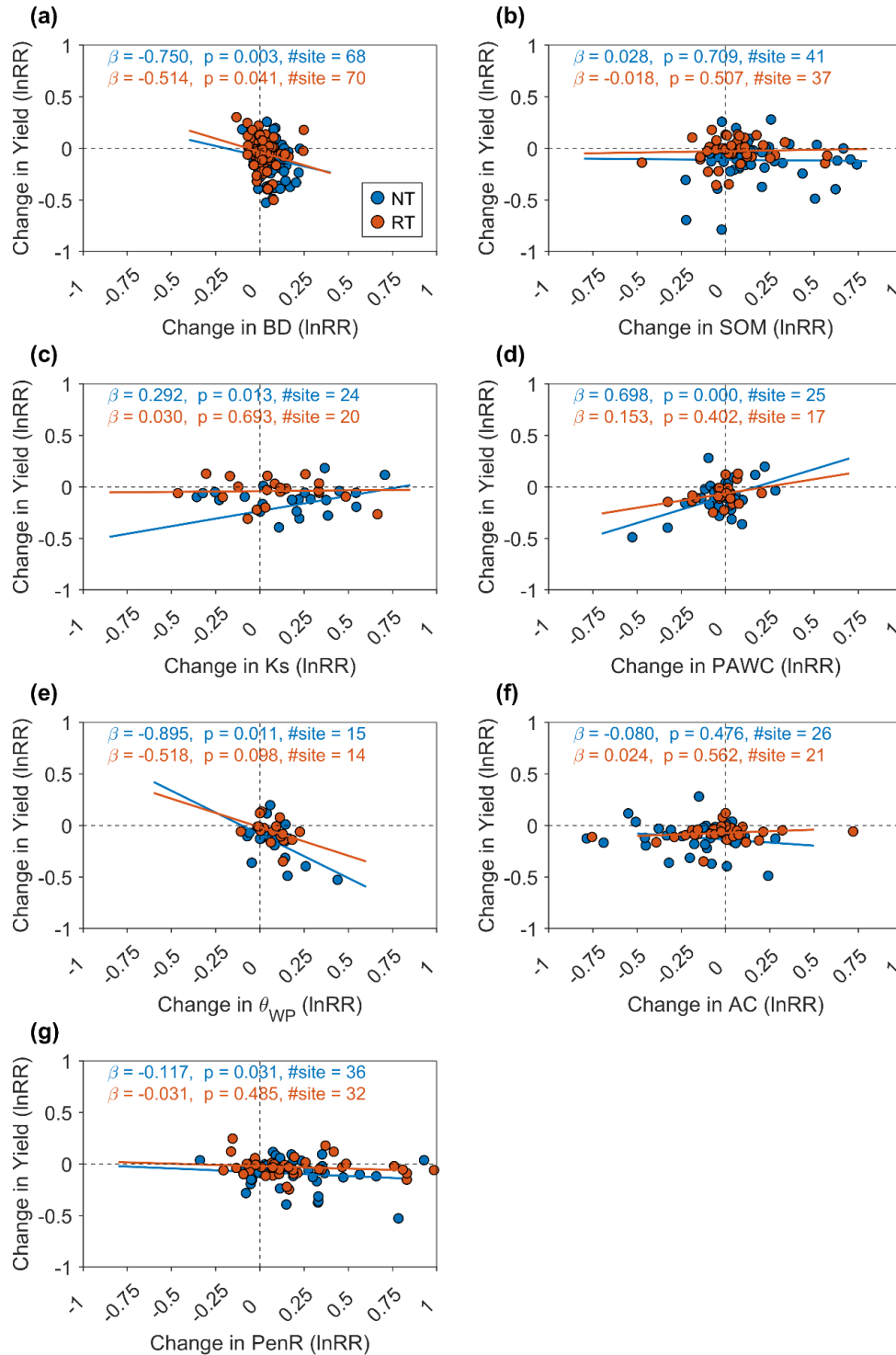
Supplementary Figure 4: Soil penetration resistance under conservation tillage and residue retention across soil depths. a) Relative effects (expressed as percentages) of no-till (NT) and reduced tillage (RT) with and without residue retention (RR) on soil penetration resistance at soil depths of 0-10 cm, 10-20 cm and 20-30 cm, compared to the control practice, conventional tillage (CT) without RR. Effect sizes were estimated using a random effect model implemented in the metafor package in R. The numbers of observations (first value) and studies (second value) from which the data were derived are shown in square brackets. Robust effects ($p < 0.05$) are shown by purple-filled circles. b) Probability distributions of penetration resistance (absolute values) under CT (dashed lines) and under NT and RT (solid lines) across the three depth intervals, based on kernel-smoothed probability density estimates.



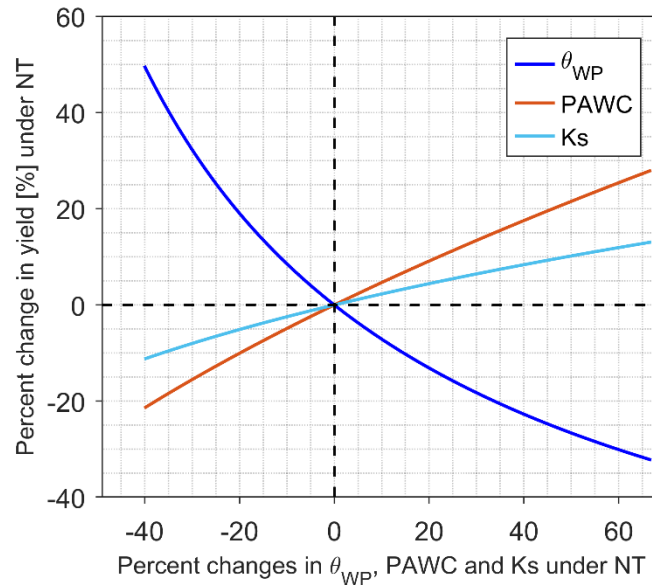
Supplementary Figure 5: Changes in plant-available water capacity (PAWC) under reduced soil disturbance and residue retention. PAWC was calculated as the difference between soil water holding capacities and field capacity and wilting point. Effects of no-till (NT) and reduced tillage (RT), with (+) and without residue retention (RR) relative to conventional tillage (CT), are shown across climatic conditions (a), soil types (b), and durations of practice (c). Climate classes were defined by the aridity index (AI) as dry (DRY; AI < 0.3), semi-dry (sDRY; 0.3 < AI ≤ 0.65) and humid (HMD; AI > 0.65). Mean effects (expressed in %) are shown by circles, with horizontal bars representing 95% confidence intervals. Dashed red vertical lines represent no effect relative to CT. Numbers in square brackets indicate the number of observations (first) and studies (second) included in each analysis. Only results based on observations from at least 5 studies are shown.



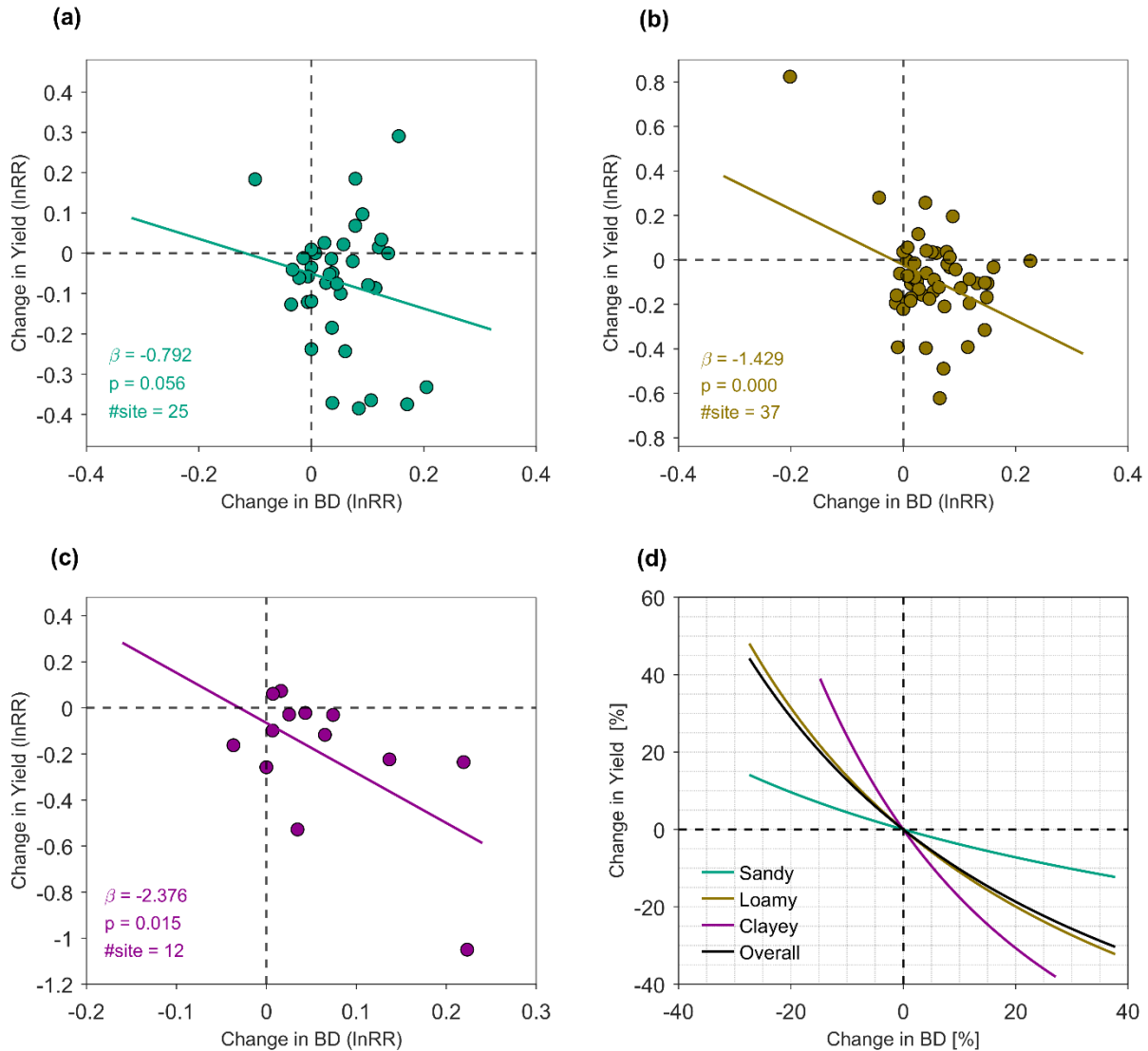
Supplementary Figure 6: Changes in air-capacity (AC) under reduced soil disturbance and residue retention. AC was calculated as the difference between soil water holding capacities and saturation and field capacity. Effects of no-till (NT) and reduced tillage (RT), with (+) and without residue retention (RR) relative to conventional tillage (CT), are shown across climatic conditions (a), soil types (b), and durations of practice (c). Climate classes were defined by the aridity index (AI) as dry (DRY; AI < 0.3), semi-dry (sDRY; 0.3 < AI ≤ 0.65) and humid (HMD; AI > 0.65). Mean effects (expressed in %) are shown by circles, with horizontal bars representing 95% confidence intervals. Cyan-filled circles show statistically significant effects. Red circles indicate statistically significant trends in the effects along gradients of climatic, soil texture or duration moderators. Dashed red vertical lines represent no effect relative to CT. Numbers in square brackets indicate the number of observations (first) and studies (second) included in each analysis. Only results based on observations from at least 5 studies are shown.



Supplementary Figure 7: Univariate mixed-effects model fitted to log-transformed response ratios (lnRR) of soil parameters and crop yield. Results are shown for a) bulk density (BD), b) soil organic matter (SOM), c) hydraulic conductivity (Kh), d) plant-available water capacity (PAWC), e) water retention at wilting point (θ_{WP}), f) air-capacity (AC), and g) penetration resistance, with yield as a response variable under no-till (NT) and reduced tillage (RT) without residue. Beta (β) denotes the model, p is the p-value of the slope, and #site indicates the number of experimental sites included in each model.



Supplementary Figure 8: Effects of changes in plant-available water capacity (PAWC), water retention at wilting point (θ_{WP}), and saturated hydraulic conductivity (K_s) on crop yield under no-till. Univariate linear mixed-effects models of log-transformed response ratios (lnRR) of observations from experimental sites where yield and soil parameters were measured simultaneously; the number of sites included in each analysis is indicated (see Supplementary Figure 7c-e). Yield lnRR was used as the response variable, soil parameters' lnRR were used as predictors, and site location was considered as a random effect. Observations were weighted by the number of replications. Model outputs were back-transformed to derive mean causal-effect curves, expressed as the percentage change in yield per percentage change in θ_{WP} and PAWC. To better visualize the effects attributable solely to the soil parameters, and to remove deviations at the origin (0,0) arising from suboptimal control (conventional tillage) practices and other factors, the mean response curves were shifted along the yield change axis so that the effect equals zero at the origin.



Supplementary Figure 9: The effects of soil bulk density on crop yield under no-till vary with soil texture. Effects were estimated using a linear mixed-effects model applied to yield and bulk density (BD) observations from experimental sites where both were available; the number of sites included in each analysis is indicated. The model consisted of the log-transformed yield response ratio (lnRR) as the response variable, log-transformed BD as the predictor, and site location ID as a random effect. Observations were weighted using a factor determined from number of replications. The slope (β) and associated p-value to indicate the strength the significance (at $\alpha = 0.05$) of BD effects on yield for three soil texture groups – (a) sandy (sand, sandy loam, loamy sand, and sandy clay loam), (b) loamy (loam, silty loam, clay loam, silty clay loam, and silt), and (c) clayey (sandy clay, clay and silty clay). Modeled effects were back-transformed to derive the mean causal-effect curves expressed as the percent change in yield per percent change in soil BD (d). To better visualize the sole causal effects of BD and to remove any deviation at the origin (0,0) due to suboptimal control (conventional tillage) practice and other factors, the mean response curve was shifted the yield change axis so that the effect is zero at the origin.

Supplementary Table 1: Univariate linear mixed-effect regression slope and p-values used for sensitivity and relative importance analysis for bulk density (BD), soil organic matter (SOM), hydraulic conductivity (Kh), plant-availability water capacity (PAWC), water retention at wilting point (θ_{WP}), air capacity (AC), and penetration resistance (PenR), under not-till (NT), reduced tillage (RT), no-till with residue retention (NT+RR), reduced tillage with residue retention (RT+RR), and conventional tillage with residue retention (CT+RR). Blank cells correspond to unavailable analysis due to insufficient data.

Soil properties	NT		RT		NT+RR		RT+RR		CT+RR	
	β	p-value	β	p-value	β	p-value	β	p-value	β	p-value
BD	-0.750	0.003	-0.514	0.041	-0.523	0.401	-1.091	0.115	-1.098	0.000
SOM	0.028	0.709	-0.018	0.507	0.067	0.633	0.397	0.021	0.439	0.045
K_s	0.292	0.013	0.030	0.693	-0.093	0.375	0.484	0.018	-0.154	0.393
PAWC	0.698	0.000	0.153	0.402	-0.594	0.111	-0.193	0.845	0.500	0.181
θ_{WP}	-0.895	0.011	-0.518	0.098	0.174	0.808	1.251	0.571	-0.188	0.871
AC	-0.080	0.476	0.024	0.562	-0.070	0.200	0.166	0.013	0.344	0.393
PenR	-0.117	0.031	-0.031	0.485	0.205	0.169	0.226	0.339	-0.096	0.783